

Model selection using time-delay lenses

Fulvio Melia,^{1*} Jun-Jie Wei,^{2,3} and Xue-Feng Wu^{2,3}

¹*Department of Physics, The Applied Math Program, and Department of Astronomy, The University of Arizona, AZ 85721, USA*

²*Purple Mountain Observatory, Chinese Academy of Sciences, Nanjing 210023, China*

³*School of Astronomy and Space Sciences, University of Science and Technology of China, Hefei 230026, China*

ABSTRACT

The sample of time-delay gravitational lenses appropriate for studying the geometry of the Universe continues to grow as dedicated campaigns, such as the Dark Energy Survey, the VST ATLAS survey, and the Large Synoptic Survey Telescope, complete their census of high-redshift sources. This catalog now includes hundreds of strong lensing systems, at least 31 of which have reasonably accurate time delay measurements. In this paper, we use them to compare the predictions of two competing Friedmann-Lemaître-Robertson-Walker models: flat Λ CDM, characterized by two adjustable parameters (H_0 and Ω_m), and the $R_h = ct$ universe (with H_0 as the single free variable). Over the past decade, the latter has accounted for the data better than the standard model, most recently the emergence of well-formed galaxies discovered by *JWST* at cosmic dawn. Here we show that the current sample of time-delay lenses favours $R_h = ct$ with a likelihood of $\sim 84\%$ versus $\sim 16\%$ for the standard model. This level of accuracy will greatly improve as the ongoing surveys uncover many thousands additional lens systems over the next several years.

Key words: cosmological parameters – cosmology: observations – cosmology: theory – gravitational lensing: strong – large-scale structure of the Universe

1 INTRODUCTION

The use of time-delay gravitational lenses to measure the expansion of the Universe has been considered for almost sixty years, starting with the original proposal by Refsdal (1964). Light rays originating from a single quasar source travel through different gravitational potentials on either side of a foreground lensing galaxy, so their deflection angles and travel times probe the model-dependent angular diameter distance from the source to the lens and the lens to the observer (Petters et al. 2001).

Of the hundreds of strong lensing systems already discovered, a small fraction of them have exhibited measurable time delays between the various images. In this paper, we assemble 31 of these with reasonably accurate data one can use for model selection. About half of the lenses have been added to the catalog only recently from the COSmological MONitoring of GRAVItational Lenses survey (COSMOGRAIL; Eigenbrod et al. 2005), the Dark Energy Survey (DES; Banerji et al. 2008; Schneider 2014), the Large Synoptic Survey Telescope (LSST; Tyson et al. 2002) project, and the VST ATLAS campaign (Koposov et al. 2014).

It is already well recognized that these strong lensing sources can yield useful constraint on the parameters in the standard model (Paraficz & Hjorth 2009; Suyu et al. 2013). For example, they may eventually help to resolve the current disagreement between the Hubble constant measured at low and high redshifts

(Rathna Kumar et al. 2015; Denzel et al. 2021). But their usefulness extends well beyond a single application to Λ CDM. They may also help with model selection via the comparative testing of quite diverse cosmologies, as we have already attempted to do using a much smaller sample (of only 12 time-delay lens systems) available back then (Wei et al. 2014).

Our analysis is motivated in part by the growing tension seen between the predictions of the standard model and the actual observations. For example, there now exists a significant disparity between the value of the Hubble constant, H_0 , inferred locally and its measurement based on the statistical analysis of anisotropies in the cosmic microwave background (CMB; Riess et al. 2022).

The Hubble constant ($= 67.4 \pm 0.5 \text{ km s}^{-1} \text{ Mpc}^{-1}$) measured by *Planck* (Planck Collaboration et al. 2020) is in 5.0σ tension with that measured using Type Ia supernovae, calibrated via the Cepheid distance ladder ($H_0 = 73.04 \pm 1.04 \text{ km s}^{-1} \text{ Mpc}^{-1}$). Other early-Universe probes, such as clustering and weak lensing, yield results similar to the CMB (Abbott et al. 2018). Measurements based on the red giant branch settle on an intermediate value of H_0 (Freedman et al. 2019, 2020). Given that the errors associated with these measurements are probably realistic (Verde et al. 2019), the implied 5.0σ disparity in the expansion of the Universe at low and high redshifts seems to refute the standard model’s predicted evolution of the Universe.

But the problems with Λ CDM extend well beyond this well-known inconsistency with H_0 . A recently published review (Melia 2023) highlights at least eight independent areas where the standard model is in significant conflict with either the observations or

* John Woodruff Simpson Fellow. E-mail: fmelia@email.arizona.edu

fundamental physical principles. A brief survey of these inconsistencies includes the initial entropy problem, an unknown classicalization process that must have converted seed quantum fluctuations into the perturbations responsible for the growth of structure, the incorrect timeline implied by the early appearance of supermassive black holes and well-formed galaxies, and the incorrect prediction of light-element abundances (notably the ${}^7\text{Li}$ anomaly) during big bang nucleosynthesis in this model.

It is therefore instructive to continue comparing the predictions of ΛCDM with those of another Friedmann-Lemaître-Robertson-Walker cosmology, known as the $R_h = ct$ universe (Melia 2007; Melia & Shevchuk 2012). Over the past 15 years, this model has been tested using over 27 different kinds of cosmological data, at both high and low redshifts, and has been favoured over the standard model by the various model selection criteria. A recent compilation of these results may be found in Table 2 of Melia (2018). Its theoretical basis and a more complete examination of its consistency with the data may be found in Melia (2020)

In this paper, we update our earlier analysis of time-delay lenses with the improved statistics offered by a sample almost three times larger than before, and examine whether our previous conclusion favouring $R_h = ct$ over ΛCDM changes as the sample size grows.

In § 2, we briefly summarize the key steps required to use time-delay lenses in cosmological testing, and then apply them to our sample of 31 systems in § 3, where we report the outcome of the one-on-one comparison between ΛCDM and $R_h = ct$. We end with our conclusion in § 4.

2 STRONG LENSING

Time-delay gravitational lenses constitute a powerful probe of the underlying cosmology, but are limited by our imprecise knowledge of the central lens mass distribution and other possible perturbing lenses along the line-of-sight. One can simplify the procedure by assembling a subsample of homogeneous systems for which one may reasonably assume the same lens model to adequately represent the mass distribution in every case (Oguri et al. 2004). Of course, we already know the selected sample is not perfectly homogeneous from the few lens systems that have been modeled independently, suggesting at least some variation in the lens structure. Taking a statistical approach, as we do here, however, can still be useful if there is a way to quantify the non-negligible dispersion arising from the poorly known systematics, which include the non-uniformity of the lens itself. We discuss how this will be done in § 3. We shall find via the use of Equation (8) that the dispersion due to this variation of the lens mass distribution appears to be smaller than $\sim 29\%$ of the measured time-delay distance (Eq. 2). While not ideal, this relatively modest inhomogeneity does present us with a workable approach we can use for model selection purposes (see § 3.2).

Let the source be located at angle $\vec{\beta}$. The time delay, Δt_i , for an image i at angular position $\vec{\theta}_i$ is due to the difference in path length along the deflected and undeflected null geodesics, as well as the gravitational time dilation incurred by the rays traversing the gravitational potential, $\Psi(\vec{\theta}_i)$, of the lens:

$$\Delta t_i = \frac{1+z_l}{c} \frac{D_A(0, z_s) D_A(0, z_l)}{D_A(z_l, z_s)} \left[\frac{1}{2} (\vec{\theta}_i - \vec{\beta})^2 - \Psi(\vec{\theta}_i) \right] \quad (1)$$

(Blandford & Narayan 1986). In this expression, z_l and z_s are the lens and source redshifts, respectively, and $D_A(z_1, z_2)$ is the angular

diameter distance between z_1 and z_2 . Thus, when the lens geometry $\vec{\theta}_i - \vec{\beta}$ and potential Ψ are known, the time delay yields the so-called time-delay distance,

$$\mathcal{R} \equiv \frac{D_A(0, z_s) D_A(0, z_l)}{D_A(z_l, z_s)}, \quad (2)$$

which clearly depends on the cosmological model.

One may find a replacement for $\Psi(\vec{\theta}_i)$ by noting that the mass distribution in lens spiral and elliptical galaxies can be represented quite well by a power-law density profile (Rusin et al. 2003), for which

$$\Psi(\vec{\theta}) = \frac{b^2}{3-n} \left(\frac{\theta}{b} \right)^{3-n}, \quad (3)$$

in terms of the deflection scale, b , and index, n . The special case with $n = 2$ is the singular isothermal sphere (SIS), with

$$b = 4\pi \frac{D_A(z_l, z_s) \sigma_\star^2}{D_A(0, z_s)}, \quad (4)$$

where σ_\star is the velocity dispersion of the lensing galaxy. Observations of the galaxy density distributions seem to suggest that n is often close to the isothermal value, so the SIS is both convenient and accurate for the majority of lens galaxies (Koopmans et al. 2009). The time delay between two images at $\vec{\theta}_A$ and $\vec{\theta}_B$ in such a lens system is given as

$$\Delta t = t_A - t_B = \frac{1+z_l}{2c} (\theta_B^2 - \theta_A^2) \mathcal{R}(z_l, z_s), \quad (5)$$

when the velocity dispersion of an SIS is assumed in these expressions. With this approach, the ‘observed’ time-delay distance is therefore inferred from the expression

$$\mathcal{R}_{\text{obs}}(z_l, z_s) = \frac{2c}{1+z_l} \frac{\Delta t}{(\theta_B^2 - \theta_A^2)}. \quad (6)$$

Of course, the actual velocity dispersion σ_\star may not match the analytical value exactly, but these do appear to be very close in the majority of lensing systems for which σ_\star has been measured (Treu et al. 2006). Nevertheless, the number of time-delay lenses for which σ_\star is known observationally is too small to make this datum useful, so all of the analysis we carry out in this paper is based solely on the use of Equation (5), though we allow for possible variations of the velocity dispersion from system to system via the introduction of a systematic error defined in Equation (8).

3 TIME-DELAY LENSES

3.1 The Sample and Methodology

Our sample of 31 time-delay gravitational lenses for which \mathcal{R}_{obs} has been ‘measured’ with Equation (5) is shown in Table 1. All of these are gravitationally lensed quasars, which show enough variability to permit an accurate measurement of a time-delay between the various images. Six of them are quadrupole image systems (RX J1131-1231, PG1115+0.80, WG0214-2105, HE0435-1223, DES J0408-5354, and WFI J2026-4536). The rest are two-image systems.

Columns 2–6 display the observational data, while column 7 lists the value of \mathcal{R}_{obs} , together with its uncertainty $\sigma_{\mathcal{R}}$. This dispersion is calculated from the statistical error using the propagation equation

$$\sigma_{\text{stat}} = \mathcal{R}_{\text{obs}} \left[\left(\frac{\sigma_{\Delta t}}{\Delta t} \right)^2 + 4 \left(\frac{\theta_B \sigma_{\theta_B}}{\theta_B^2 - \theta_A^2} \right)^2 + 4 \left(\frac{\theta_A \sigma_{\theta_A}}{\theta_B^2 - \theta_A^2} \right)^2 \right]^{1/2}, \quad (7)$$

Table 1. Time Delay Lenses

System	z_l	z_s	θ_A (arcsec)	θ_B (arcsec)	$\Delta t = t_A - t_B$ (days)	\mathcal{R}_{obs} (with $\eta = 0.29$) (Gpc)	$\mathcal{R}_{R_h=ct}$ (Gpc)	$\mathcal{R}_{\Lambda\text{CDM}}$ (Gpc)	Refs.
FBQ0951+2635	0.26	1.246	0.886 ± 0.004	0.228 ± 0.008	-16.0 ± 2.0	1.238 ± 0.391	0.947	0.927	6
SDSS J1442+4055	0.284	2.593	1.385 ± 0.049	0.771 ± 0.028	-25.0 ± 1.5	1.051 ± 0.331	0.893	0.889	36, 37
RX J1131-1231	0.295	0.657	1.898 ± 0.015	1.922 ± 0.023	1.6 ± 0.7	0.963 ± 1.215	1.509	1.469	21, 39
PG1115+0.80	0.311	1.722	1.12 ± 0.014	0.95 ± 0.016	-8.3 ± 1.5	1.286 ± 0.467	1.045	1.036	32, 33
QJ0158-4325	0.317	1.29	0.814 ± 0.038	0.41 ± 0.02	-22.7 ± 3.6	2.491 ± 0.884	1.156	1.141	21, 40
Q0957+561	0.36	1.413	5.220 ± 0.006	1.036 ± 0.11	-417.09 ± 0.07	0.837 ± 0.243	1.282	1.272	6, 13, 14
HS0818+1227	0.39	3.113	2.219 ± 0.009	0.615 ± 0.003	-153.8 ± 13.9	1.740 ± 0.529	1.140	1.152	21
SDSS J0924+0219	0.393	1.523	0.878 ± 0.021	0.977 ± 0.072	2.4 ± 3.8	0.671 ± 1.203	1.368	1.363	21, 41, 6
SDSS J1620+1203	0.398	1.158	2.277 ± 0.037	0.494 ± 0.01	-171.5 ± 8.7	1.775 ± 0.526	1.567	1.552	21, 42
DES2325-5229	0.400	2.74	1.23 ± 0.05	1.79 ± 0.05	43.8 ± 4.3	1.322 ± 0.439	1.191	1.201	24, 46
HE0047-1756	0.407	1.678	0.894 ± 0.043	0.553 ± 0.027	-10.4 ± 3.5	1.071 ± 0.508	1.371	1.370	21, 24, 38
B1600+434	0.414	1.589	1.14 ± 0.075	0.25 ± 0.074	-51.0 ± 4.0	2.084 ± 0.692	1.422	1.421	4, 5, 20
J1001+5027	0.415	1.838	1.98 ± 0.08	0.93 ± 0.19	-119.3 ± 3.3	1.972 ± 0.651	1.357	1.360	30, 31
SDSS J1335+0118	0.44	1.570	1.079 ± 0.031	0.489 ± 0.014	-56.0 ± 5.9	3.004 ± 0.954	1.523	1.524	21, 48
WG0214-2105	0.45	3.24	1.018 ± 0.225	1.246 ± 0.275	7.5 ± 2.8	0.716 ± 1.193	1.273	1.296	24, 47
HE0435-1223	0.454	1.693	1.298 ± 0.008	1.168 ± 0.014	-9.0 ± 0.8	1.380 ± 0.451	1.527	1.533	21, 6
Q0142-100	0.491	2.73	1.855 ± 0.002	0.383 ± 0.005	-97 ± 15.8	1.411 ± 0.469	1.419	1.445	6, 12, 21
SDSS J1650+4251	0.577	1.547	0.872 ± 0.027	0.357 ± 0.042	-49.5 ± 1.9	3.544 ± 1.083	2.079	2.102	6, 18
DES J0408-5354	0.597	2.375	3.626 ± 0.342	3.053 ± 0.361	112.1 ± 2.1	1.311 ± 1.199	1.758	1.802	26, 43
HE2149-2745	0.603	2.033	1.354 ± 0.008	0.344 ± 0.012	-72.6 ± 17.0	1.887 ± 0.704	1.890	1.929	6, 9, 21, 49
SDSS J1339+1310	0.609	2.231	0.580 ± 0.041	1.234 ± 0.106	47.0 ± 5.5	1.760 ± 0.677	1.835	1.879	34, 35
SDSS J0832+0404	0.659	1.116	1.56 ± 0.024	0.435 ± 0.008	-125.3 ± 18.2	2.405 ± 0.784	3.469	3.494	21, 45
B0218+357	0.685	0.944	0.057 ± 0.004	0.280 ± 0.008	$+11.3 \pm 0.2$	6.378 ± 1.892	5.312	5.313	1, 2, 3, 19
Q1355-2257	0.702	1.370	0.959 ± 0.081	0.267 ± 0.023	-81.5 ± 11.6	4.034 ± 1.500	3.005	3.052	21, 6
SBS1520+530	0.717	1.855	1.207 ± 0.004	0.386 ± 0.008	-130.0 ± 3.0	4.137 ± 1.204	2.397	2.460	6, 16
HE1104-1805	0.729	2.319	1.099 ± 0.004	2.095 ± 0.008	152.2 ± 3.0	1.978 ± 0.575	2.150	2.223	2, 7, 8
SDSS J1515+1511	0.742	2.054	1.676 ± 0.104	0.313 ± 0.019	-210.2 ± 5.6	3.181 ± 1.013	2.338	2.411	21, 44
SDSS J1206+4332	0.748	1.789	1.870 ± 0.088	1.278 ± 0.097	-111 ± 3	2.435 ± 0.891	2.588	2.659	17, 23
SBS0909+532	0.83	1.377	0.415 ± 0.126	0.756 ± 0.152	$+50.0 \pm 3.0$	4.890 ± 3.415	4.034	4.127	6, 15, 22
PKS1830-211	0.89	2.507	0.67 ± 0.08	0.32 ± 0.08	-26.0 ± 5.0	2.837 ± 1.386	2.523	2.640	10, 11
WFI J2026-4536	1.04	2.23	0.673 ± 0.156	0.801 ± 0.184	18.7 ± 4.8	3.472 ± 6.795	3.290	3.464	21, 6

References: (1) Carilli et al. (1993); (2) Lehár et al. (2000); (3) Wucknitz et al. (2004); (4) Jackson et al. (1995); (5) Dai & Kochanek (2005); (6) Kochanek et al. (2008); (7) Wisotzki et al. (1993); (8) Poindexter et al. (2007); (9) Burud et al. (2002); (10) Lovell et al. (1998); (11) Meylan et al. (2005); (12) Koptelova et al. (2012); (13) Falco et al. (1997); (14) Colley et al. (2003); (15) Dai & Kochanek (2009); (16) Auger et al. (2008); (17) Paraficz & Hjorth (2009); (18) Vuissoz et al. (2007); (19) Biggs & Browne (2018); (20) Burud et al. (2000); (21) Millon et al. (2020); (22) Hainline et al. (2013); (23) Eulaers et al. (2013); (24) Millon et al. (2020); (25) Koopmans et al. (2003); (26) Courbin et al. (2018); (27) Eulaers & Magain (2011); (28) Fohlmeister et al. (2008); (29) Bonvin et al. (2019); (30) Rathna Kumar et al. (2013); (31) Oguri et al. (2005); (32) Bonvin et al. (2018); (33) Morgan et al. (2008); (34) Goicoechea & Shalyapin (2016); (35) Inada et al. (2009); (36) Shalyapin & Goicoechea (2019); (37) Sergeev et al. (2016); (38) Wisotzki et al. (2004); (39) Sluse et al. (2007); (40) Morgan et al. (2008); (41) Inada et al. (2003); (42) Kayo et al. (2010); (43) Agnello et al. (2017); (44) Inada et al. (2014); (45) Oguri et al. (2008); (46) Ostrovski et al. (2017); (47) Spiniello et al. (2019); (48) Oguri et al. (2004); (49) Rathna Kumar et al. (2015).

and a second source of (systematic) error, σ_{sys} , that takes into account various effects giving rise to the observed scatter of individual lenses from the assumed pure SIS profile. These include a possible rms deviation of the lens velocity dispersion, a steepening of the mean mass density profile compared to that of a pure SIS (Koopmans et al. 2009), and the non-zero line-of-sight contribution, which is non-zero on average.

According to Cao et al. (2012), σ_{sys} may be as large as $\sim 20\%$. Since we don't know how large this error is a priori, we model it along with the other variables in our maximum likelihood analysis and write it as

$$\sigma_{\text{sys}} \equiv \eta \mathcal{R}_{\text{obs}}, \quad (8)$$

in terms of the additional free parameter η . Its introduction is just a convenient way to characterize this systematic uncertainty in terms of the value of \mathcal{R}_{obs} . In our maximum likelihood estimation, this additional free parameter is optimized along with the other free parameters individually for each model being tested. As we shall see

below, however, η appears to be quite independent of the cosmology itself, and turns out to have the value $\eta = 0.29^{+0.06}_{-0.05}$ (1σ) for the sample of 31 lens systems used in this study, consistent with the earlier finding of Cao et al. (2012). The total uncertainty $\sigma_{\mathcal{R}}$ in \mathcal{R}_{obs} is then found by adding σ_{stat} and σ_{sys} in quadrature,

$$\sigma_{\mathcal{R}}^2 = \sigma_{\text{stat}}^2 + \sigma_{\text{sys}}^2, \quad (9)$$

and this is the error appearing in column 7 of Table 1.

Columns 8 and 9 in this table display the optimized model predictions for $R_h = ct$ and ΛCDM , respectively, which we now describe. The angular-diameter distance in ΛCDM is a function of several parameters, including H_0 and the mass fractions $\Omega_m \equiv \rho_m/\rho_c$, $\Omega_{\text{de}} \equiv \rho_{\text{de}}/\rho_c$, and $\Omega_r \equiv \rho_r/\rho_c$, for matter, dark energy and radiation, respectively, defined as ratios of the critical density $\rho_c \equiv 3c^2 H_0^2 / 8\pi G$. To streamline the optimization of the fit with this model, we adopt a minimal number of unknown variables, so we assume that dark energy is a cosmological constant ($\Omega_{\text{de}} = \Omega_\Lambda$), and that the spatial curvature constant is zero. In that case, since the contribution from radiation in the redshift range covered in Ta-

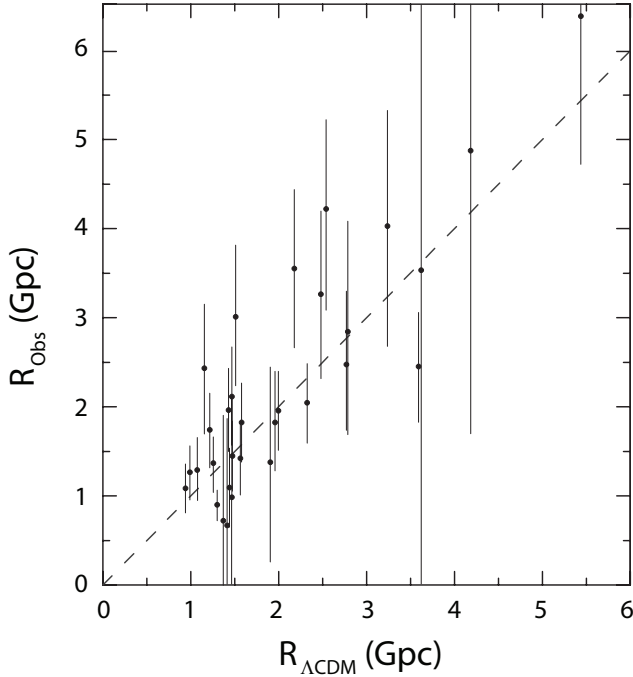


Figure 1. Thirty one \mathcal{R} measurements, with error bars, compared to the predictions of Λ CDM, with optimized parameters: $H_0 = 85.6^{+7.0}_{-5.9}$ (1σ) $\text{km s}^{-1} \text{Mpc}^{-1}$, $\Omega_m = 0.50^{+0.34}_{-0.34}$ (1σ) and $\eta = 0.29^{+0.06}_{-0.05}$ (1σ) (see Fig. 2). The dashed line indicates a perfect match between theory and observation. The reduced χ^2 for this fit is 0.971 (28 dof).

ble 1 is insignificant compared to that of the others, we simply put $\Omega_m + \Omega_\Lambda = 1$. Then, the angular-diameter distance between redshifts z_1 and z_2 ($> z_1$) is given by the expression

$$D_A^{\Lambda\text{CDM}}(z_1, z_2) = \frac{c}{H_0} \frac{1}{(1+z_2)} \int_{z_1}^{z_2} \frac{dz}{[\Omega_m(1+z)^3 + \Omega_\Lambda]^{1/2}}. \quad (10)$$

With this application of the standard model, we thus have three free parameters in total for the optimization: the cosmological parameters H_0 and Ω_m , and the time-delay lens dispersion parameter η .

On the other hand, the angular-diameter distance in $R_h = ct$ (Melia 2007; Melia & Shevchuk 2012; Melia 2020) depends only on H_0 :

$$D_A^{R_h=ct}(z_1, z_2) = \frac{c}{H_0} \frac{1}{(1+z_2)} \ln\left(\frac{1+z_2}{1+z_1}\right). \quad (11)$$

To find the best fit to the data in Table 1, we therefore optimize two free parameters for this model: H_0 and η .

For each model, we optimize the fit by maximizing the joint likelihood function

$$L(\sigma_{\mathcal{R}}, \xi) \propto \prod_{i=1} \frac{1}{\sigma_{\mathcal{R}_i}} \exp\left[-\frac{(\mathcal{R}_i[\xi] - \mathcal{R}_{\text{obs},i})^2}{2\sigma_{\mathcal{R}_i}^2}\right], \quad (12)$$

where $\mathcal{R}_i[\xi]$ is the theoretical prediction of the time-delay distance between $z_{l,i}$ and $z_{s,i}$ for either Λ CDM or $R_h = ct$ and the model specific parameters ξ , $\mathcal{R}_{\text{obs},i}$ is the measured value, and $\sigma_{\mathcal{R}_i}$ is the dispersion of $\mathcal{R}_{\text{obs},i}$ given in Equation (9).

We follow this procedure using the data in Table 1 with the restriction $0.0 \leq \Omega_m \leq 1.0$, and find that Λ CDM fits the observed time-delay distances with a maximum likelihood corresponding to the parameter values $H_0 = 85.6^{+7.0}_{-5.9}$ (1σ) $\text{km s}^{-1} \text{Mpc}^{-1}$, $\Omega_m = 0.50^{+0.34}_{-0.34}$ (1σ) and $\eta = 0.29^{+0.06}_{-0.05}$ (1σ). The best fit with the $R_h = ct$ universe is provided by the optimized parameters $H_0 = 81.3^{+6.5}_{-5.4}$

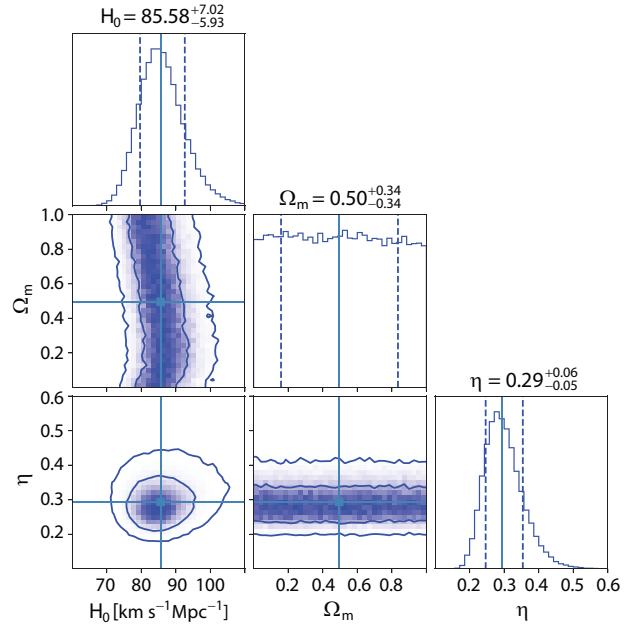


Figure 2. 1D probability distributions and 2D regions with 1σ and 2σ contours for the best-fit Λ CDM model (see Fig. 1).

(1σ) $\text{km s}^{-1} \text{Mpc}^{-1}$ and $\eta = 0.29^{+0.06}_{-0.05}$ (1σ). The 1σ and 2σ confidence intervals for these model are shown in Figures 2 and 4, and the entries in columns 8 and 9 of Table 1 correspond to these best-fit parameters.

These results confirm a feature of the fit with Λ CDM reported on several previous occasions (Coe & Moustakas 2009; Linder 2011; Treu & Marshall 2016). The principal dependence of the time-delay distance (Eq. 2) is on the Hubble constant, H_0 , to which it is inversely proportional. The impact of a variation of Ω_m on the ratio of angular-diameter distances in this expression is much weaker. One therefore needs a much bigger sample to constrain Ω_m very tightly.

The observed values \mathcal{R}_{obs} are displayed in Figures 1 and 3, in comparison with those predicted by the two models. In these plots, a perfect match would correspond to the straight dashed line. The clustering of points towards small values of \mathcal{R} reflects the preponderance of lenses at relatively small redshifts. Interestingly, the optimized value of η is the same in both models, suggesting that the systematics are independent of the cosmology and do indeed represent an intrinsic dispersion of the lens potential away from a pure SIS. With its inclusion in the overall error budget, we find that both models fit this sample of 31 time-delay lenses quite well. The reduced χ^2 is 0.971 (28 dof) for Λ CDM in Figure 1, and a slightly better 0.937 (29 dof) for $R_h = ct$ in Figure 3.

3.2 Model Selection

Since these models formulate the angular-diameter distance in Equations (10) and (11) differently, however, without the same number of free parameters, a comparison of the likelihoods to determine which of them is favoured by the data needs to be based on model selection tools. To compare the evidence for and against competing models, the use of information criteria has become quite common in cosmology (see, e.g., Takeuchi 2000; Liddle 2004, 2007; Tan & Biswas 2012; Schwarz 1978). Such a tool may be

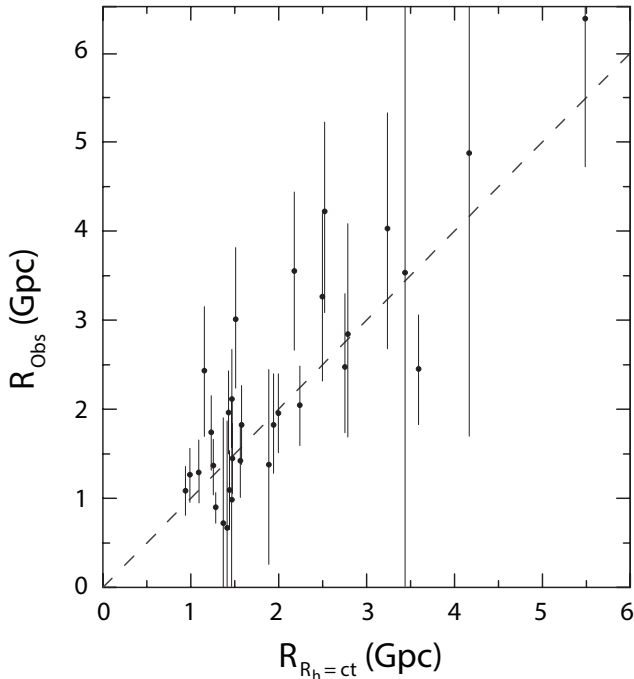


Figure 3. Same as Fig. 1, except now for the $R_h = ct$ universe, with optimized parameters: $H_0 = 81.3^{+6.5}_{-5.4}$ (1σ) $\text{km s}^{-1} \text{Mpc}^{-1}$ and $\eta = 0.29^{+0.06}_{-0.05}$ (1σ) (see Fig. 4). The reduced χ^2 for this fit is 0.937 (29 dof).

viewed as an enhanced ‘goodness of fit’ criterion, extending the usual χ^2 diagnostic by including the number of free parameters in each model. The information criteria favour models with fewer parameters over those with many, as long as the latter do not provide a considerably better fit to the data.

An information criterion provides the relative ranks of two or more competing models, along with a numerical estimate of confidence that each is the best, analogous to the likelihood (or posterior probability) in traditional statistical inference. Information criteria are superior to the latter, however, in that they can be applied to models that are not ‘nested,’ providing a procedure for comparing candidates that are not specializations of each other.

An information criterion can be applied after the following kind of regression is performed. Suppose that corresponding to the values z_1, \dots, z_N of a free parameter the measured values are h_1, \dots, h_N of a dependent one, with (known) error bars $\pm\sigma_1, \dots, \pm\sigma_N$. These errors are assumed to be normally distributed. Now let a model \mathcal{M} predict values $\hat{h}_1, \dots, \hat{h}_N$, inferred from a formula $\hat{h}_i = \hat{h}_i(\vec{\beta})$ involving a parameter vector $\vec{\beta}$ comprising f unknown variables, i.e., $\vec{\beta} = (\beta_1, \dots, \beta_f)$. In other words, the data model \mathcal{M} is in effect a statistical one, of the form

$$h_i = \hat{h}_i(\vec{\beta}) + \sigma_i Z_i, \quad (13)$$

where Z_1, \dots, Z_N are independent standard normal random variables. Note that in the case of linear regression, $\hat{h}_i(\vec{\beta})$ would be $\sum_{j=1}^f X_{ij}\beta_j$ for known coefficients X_{ij} . Typically, $X_{ij} = \hat{h}^{(j)}(z_i)$ for known functions $\hat{h}^{(1)}, \dots, \hat{h}^{(f)}$ of z .

Then for model \mathcal{M} , the χ^2 goodness of fit to the data is expressible as

$$\chi^2 = \sum_{i=1}^N [h_i - \hat{h}_i(\vec{\beta})]^2 / \sigma_i^2, \quad (14)$$

i.e., a (weighted) sum of squared errors, and the χ^2 per degree of

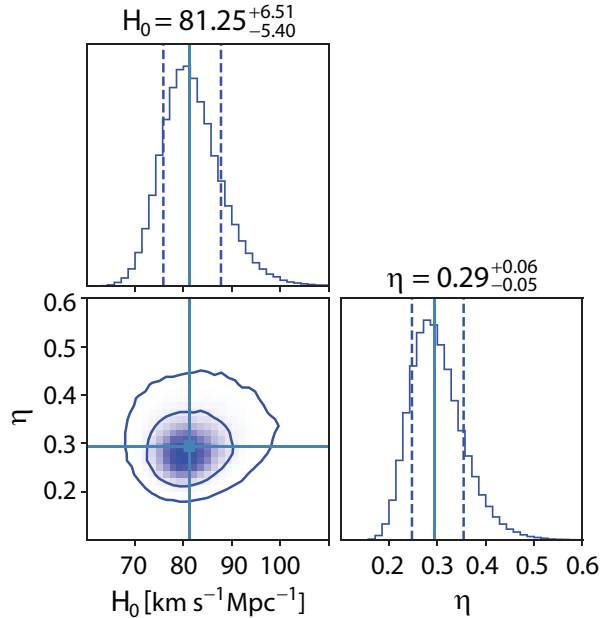


Figure 4. Same as Fig. 2, except now for the $R_h = ct$ universe, whose best fit is shown in Fig. 3.

freedom,

$$\chi^2_{\text{dof}} = \chi^2 / (N - f). \quad (15)$$

By necessity, we must also have $N > f$. The parameters $(\beta_1, \dots, \beta_f)$ are selected to minimize the χ^2 , producing a best fit to the data.

For the data we use in this paper, the sample is large (i.e., > 20), so the most appropriate one to use is the Bayesian Information Criterion (BIC; Schwarz 1978), which tests the statistical performance of the models. It is defined as

$$\text{BIC} \equiv -2 \ln L + (\ln N) f \quad (16)$$

where, as previously noted, N is the number of data points (here 31) and f is the number of free parameters (three for ΛCDM and two for $R_h = ct$).

The BIC is generally considered to be a large-sample ($N \gg 1$) approximation to the outcome of a conventional Bayesian inference procedure for selecting the model preferred by the data. Among the available choices being tested, the model with the lowest BIC score is the one selected by this criterion. Among its many proponents, Liddle (2007) has argued for the use of BIC in cosmological model selection, which has now been done to compare several popular models against ΛCDM (see, e.g., Shi et al. 2012).

Two statistical models of the data set (h_1, \dots, h_N) , such as a ‘true’ model \mathcal{M}_* and a second model \mathcal{M} , may be viewed as probability density functions (PDF’s) on \mathbb{R}^N , say $F_*(h_1, \dots, h_N)$ and $F(h_1, \dots, h_N)$, respectively. In information theory, the discrepancy of the PDF F from the PDF F_* —effectively, a measure of distance—is given by the Kullback–Leibler formula

$$D(\mathcal{M}_* \parallel \mathcal{M}) = \int_{\mathbb{R}^n} dh_1 \dots dh_n F_*(h) \ln \frac{F_*(h)}{F(h)} \geq 0 \quad (17)$$

(using the notation that the argument h stands for the entire data set $[h_1, \dots, h_N]$). The best model \mathcal{M} may be selected from a set of candidate models by choosing the one with the minimum $D(\mathcal{M}_* \parallel \mathcal{M})$. The model \mathcal{M}_* is not known, but the \mathcal{M} with parameters optimized

by minimizing χ^2 , is special. It turns out that the BIC of the fitted model \mathcal{M} approximates $2D(\mathcal{M}_*||\mathcal{M})$, up to an unimportant additive constant. This is especially true when \mathcal{M}_* is a model of the same type, with free variables $(\beta_1^*, \dots, \beta_f^*)$.

The quantity BIC/2 is an unbiased estimator of the distance $D(\mathcal{M}_*||\mathcal{M})$. This statement is exact for linear regression, and correct to leading order for non-linear regression. The fitted model \mathcal{M} does depend on the data set, so both $D(\mathcal{M}_*||\mathcal{M})$ and BIC/2 are random variables. In the language of probability, a lack of bias translates to them having the same expectation.

The extent to which the fitted information criteria represent an *accurate* estimate of $2D(\mathcal{M}_*||\mathcal{M})$ has been investigated theoretically (see, e.g., Yanagihara & Ohmoto 2005). Their variability has also been studied by repeatedly comparing Λ CDM to other cosmological models (Tan & Biswas 2012). In the case of BIC, it is known that the magnitude of the difference $\Delta = \text{BIC}_2 - \text{BIC}_1$ provides a numerical assessment of the evidence that model 1 is preferred over model 2. As a general rule, the evidence is considered to be weak if $\Delta \lesssim 2$, mildly strong if $\Delta \approx 3$ or 4, and quite strong if $\Delta \gtrsim 5$.

One may thus rank the competing models quantitatively as follows. If BIC_α characterizes model α , the unnormalized confidence that this model is correct is the ‘Bayes weight’ $\exp(-\text{BIC}_\alpha/2)$. The likelihood of model α being correct relative to the others is then

$$P(\alpha) = \frac{\exp(-\text{BIC}_\alpha/2)}{\sum_i \exp(-\text{BIC}_i/2)}. \quad (18)$$

The sum in the denominator includes all of the candidates being tested simultaneously.

The outcome of this analysis shows that $R_h = ct$ is preferred over Λ CDM with a $-2 \ln L = 444.73$ versus 444.68 (or equivalently, with a BIC = 451.60 versus 454.98), which translates into a probability of $\sim 84\%$ versus $\sim 16\%$ of being the correct model. To complete the discussion, we also considered how well the time-delay lens data are fit by *Planck* Λ CDM, i.e., the version of the standard model with its parameters fixed at the values optimized by *Planck* (Planck Collaboration et al. 2020): $H_0 = 67.4 \text{ km s}^{-1} \text{ Mpc}^{-1}$ and $\Omega_m = 0.315$. Not surprisingly, a head-to-head comparison between this model and $R_h = ct$ reveals a much more slanted result, with the latter being favoured by these data with a probability of $\sim 99.3\%$ versus only $\sim 0.7\%$.

4 CONCLUSION

Our use of a much larger time-delay lens sample (31) compared to the set of 12 systems we used in our first attempt to carry out this kind of analysis (Wei et al. 2014), has refined the parameter search and reduced their 1σ errors, but the optimized values themselves have changed very little. For example, the updated value of H_0 in the context of Λ CDM is now $85.6^{+7.0}_{-5.9} (1\sigma) \text{ km s}^{-1} \text{ Mpc}^{-1}$ compared with $87^{+17}_{-16} (1\sigma) \text{ km s}^{-1} \text{ Mpc}^{-1}$. But the intrinsic dispersion (as measured by the parameter η) persists, as indicated by its current value, $\eta = 0.29^{+0.06}_{-0.05} (1\sigma)$, versus $\eta = 0.29^{+0.15}_{-0.09} (1\sigma)$. As noted earlier, this suggests that the poorly known systematics are probably due solely to deviations of the lens potential from a pure SIS, as opposed to any cosmological influence.

Overall, our analysis of the time-delay distances using a larger sample size has affirmed our earlier conclusion that $R_h = ct$ is favoured by these data over the current standard model. This catalog of lens systems is expected to grow considerably over the coming years, improving the statistics even further and motivating a

more realistic handling of the lens mass distribution in order to mitigate the impact of σ_{sys} well below the current limitations.

In our previous work (Wei et al. 2014), we estimated that if the real cosmology is Λ CDM, one would need a sample of ~ 150 time-delay lenses to rule out $R_h = ct$ at a confidence level of $\sim 99.7\%$, while ~ 1000 lenses would be required to rule out Λ CDM if the actual universe were instead $R_h = ct$. This difference is due to the greater flexibility afforded the standard model by its greater number of free parameters.

Looking forward, the prospects of attaining a sample of this size look quite promising. Several ongoing and future survey programs include a search for strong lensing systems in their purview. According to some estimates, the Large-aperture Synoptic Survey Telescope (LSST) will observe some 8000 lensed quasars during its 10-year lifetime, about 3000 of which will have well-measured time-delays (Oguri & Marshall 2010; Collett 2015). A subsample useful for a detailed analysis based on the modelling of individual lenses would require an accurate characterization of the mass distribution of the lens galaxy, auxiliary data including high-resolution imaging, and measurements of the stellar velocity distribution. Such requirements would reduce the sample of strong gravitational lenses with accurate time-delay measurements to ~ 100 . With the statistical approach we have used in this paper, however, in contrast to individual modelling, the latter requirements may generally be waived, allowing us to expect a usable sample approaching 1000 or more new (LSST) lenses for future work.

But LSST is not the only survey mission promising to increase the sample size. *Euclid* may provide a comparable number (Jee et al. 2016; Laureijs et al. 2011), and the *DESI* Legacy Imaging Survey has already started reporting the discovery of over 1000 new strong lensing candidates (most of which are galaxy-galaxy pairs, rather than quasar-galaxy systems). Future work is expected to uncover many thousands more (Huang et al. 2022). The Square Kilometer Array (SKA) will in addition be able to compile up to $\sim 10^5$ lensing systems with $\sim 100\%$ reliability and known source redshifts (Laureijs et al. 2011). Several hundred new candidates have also been reported by the (HOLISMOKES) Hyper Suprime-Cam (HSC) survey, with thousands more expected with continued imaging (Cañameras et al. 2021).

Our expectation is that the requisite number of strong lensing systems with accurate time-delay measurements to rule out $R_h = ct$ if the real cosmology is Λ CDM should be attainable in just a few years. Compiling a sample of ~ 1000 such systems to rule out Λ CDM if the real cosmology is instead $R_h = ct$ will take longer, but is nevertheless quite feasible during this decade with the combined efforts of the many ongoing and future survey missions.

ACKNOWLEDGMENTS

We are very grateful to the anonymous referee for their excellent review of this paper and for making several suggestions to improve its presentation. This work is partially supported by the National Key Research and Development Program of China (2022SKA0130100), the National Natural Science Foundation of China (grant Nos. 11725314 and 12041306), the Key Research Program of Frontier Sciences (grant No. ZDBS-LY-7014) of Chinese Academy of Sciences, and the Natural Science Foundation of Jiangsu Province (grant No. BK20221562).

DATA AVAILABILITY STATEMENT

No new data were generated or analysed in support of this research.

REFERENCES

- Abbott T. M. C., Abdalla F. B., Annis J., Bechtol K., Blazek J., Benson B. A., Bernstein R. A., Bernstein G. M., Bertin E., Brooks D., Burke D. L., Carnero Rosell A., et al. South Pole Telescope Collaboration 2018, *MNRAS*, 480, 3879
- Agnello A., Lin H., Buckley-Geer L., Treu T., Bonvin V., Courbin F., Lemon C., Morishita T., Amara A., Auger M. W., Birrer S., et al. 2017, *MNRAS*, 472, 4038
- Auger M. W., Fassnacht C. D., Wong K. C., Thompson D., Matthews K., Soifer B. T., 2008, *ApJ*, 673, 778
- Banerji M., Abdalla F. B., Lahav O., Lin H., 2008, *MNRAS*, 386, 1219
- Biggs A. D., Browne I. W. A., 2018, *MNRAS*, 476, 5393
- Blandford R., Narayan R., 1986, *ApJ*, 310, 568
- Bonvin V., Chan J. H. H., Millon M., Rojas K., Courbin F., Chen G. C. F., Fassnacht C. D., Paic E., Tewes M., Chao D. C. Y., Chijani M., et al. 2018, *A&A*, 616, A183
- Bonvin V., Millon M., Chan J. H. H., Courbin F., Rusu C. E., Sluse D., Suyu S. H., Wong K. C., Fassnacht C. D., Marshall P. J., Treu T., et al. 2019, *A&A*, 629, A97
- Burud I., Courbin F., Magain P., Lidman C., Hutsemékers D., Kneib J. P., Hjorth J., Brewer J., Pompei E., Germany L., Pritchard J., Jaunsen A. O., Letawe G., Meylan G., 2002, *A&A*, 383, 71
- Burud I., Hjorth J., Jaunsen A. O., Andersen M. I., Korhonen H., Clasen J. W., Pelt J., Pijpers F. P., Magain P., Østensen R., 2000, *ApJ*, 544, 117
- Cañameras R., Schuldt S., Shu Y., Suyu S. H., Taubenberger S., Meinhardt T., Leal-Taixé L., Chao D. C. Y., Inoue K. T., Jaelani A. T., More A., 2021, *A&A*, 653, L6
- Cao S., Pan Y., Biesiada M., Godlowski W., Zhu Z.-H., 2012, *Journal of Cosmology and Astro-Particle Physics*, 2012, 016
- Carilli C. L., Rupen M. P., Yanny B., 1993, *ApJ Letters*, 412, L59
- Coe D., Moustakas L. A., 2009, *ApJ*, 706, 45
- Collett T. E., 2015, *ApJ*, 811, 20
- Colley W. N., Schild R. E., Abajas C., Alcalde D., Aslan Z., Bikmaev I., Chavushyan V., Chinarró L., Cournoyer J.-P., Crowe R., et al. 2003, *ApJ*, 587, 71
- Courbin F., Bonvin V., Buckley-Geer E., Fassnacht C. D., Frieman J., Lin H., Marshall P. J., Suyu S. H., Treu T., Angueta T., Motta V., et al. 2018, *A&A*, 609, A71
- Dai X., Kochanek C. S., 2005, *ApJ*, 625, 633
- Dai X., Kochanek C. S., 2009, *ApJ*, 692, 677
- Denzel P., Coles J. P., Saha P., Williams L. L. R., 2021, *MNRAS*, 501, 784
- Eigenbrod A., Courbin F., Vuissoz C., Meylan G., Saha P., Dye S., 2005, *A&A*, 436, 25
- Eulaers E., Magain P., 2011, *A&A*, 536, A44
- Eulaers E., Tewes M., Magain P., Courbin F., Asfandiyarov I., Ehgamberdiev S., Rathna Kumar S., Stalin C. S., Prabhu T. P., Meylan G., Van Winckel H., 2013, *A&A*, 553, A121
- Falco E. E., Shapiro I. I., Moustakas L. A., Davis M., 1997, *ApJ*, 484, 70
- Fohlmeister J., Kochanek C. S., Falco E. E., Morgan C. W., Wambsganss J., 2008, *ApJ*, 676, 761
- Freedman W. L., Madore B. F., Hatt D., Hoyt T. J., Jang I. S., Beaton R. L., Burns C. R., Lee M. G., Monson A. J., Neeley J. R., Phillips M. M., Rich J. A., Seibert M., 2019, *ApJ*, 882, 34
- Freedman W. L., Madore B. F., Hoyt T., Jang I. S., Beaton R., Lee M. G., Monson A., Neeley J., Rich J., 2020, *ApJ*, 891, 57
- Goicoechea L. J., Shalyapin V. N., 2016, *A&A*, 596, A77
- Hainline L. J., Morgan C. W., MacLeod C. L., Landaal Z. D., Kochanek C. S., Harris H. C., Tillemann T., Goicoechea L. J., Shalyapin V. N., Falco E. E., 2013, *ApJ*, 774, 69
- Huang X., Storfer C., Gu A., Ravi V., Pilon A., Sheu W., Venguswamy R., Banka S., Dey A., Landriau M., Lang D., et al. 2022, *VizieR Online Data Catalog*, p. J/ApJ/909/27
- Inada N., Becker R. H., Burles S., Castander F. J., Eisenstein D., Hall P. B., Johnston D. E., Pindor B., Richards G. T., Schechter P. L., Sekiguchi M., et al. 2003, *Astronomical Journal*, 126, 666
- Inada N., Oguri M., Rusu C. E., Kayo I., Morokuma T., 2014, *Astronomical Journal*, 147, 153
- Inada N., Oguri M., Shin M.-S., Kayo I., Strauss M. A., Morokuma T., Schneider D. P., Becker R. H., Bahcall N. A., York D. G., 2009, *Astronomical Journal*, 137, 4118
- Jackson N., de Bruyn A. G., Myers S., Bremer M. N., Miley G. K., Schilizzi R. T., Browne I. W. A., Nair S., Wilkinson P. N., Blandford R. D., Pearson T. J., Readhead A. C. S., 1995, *MNRAS*, 274, L25
- Jee I., Komatsu E., Suyu S. H., Huterer D., 2016, *JCAP*, 2016, 031
- Kayo I., Inada N., Oguri M., Morokuma T., Hall P. B., Kochanek C. S., Schneider D. P., 2010, *Astronomical Journal*, 139, 1614
- Kochanek C. S., Falco E. E., Impey C., et al., 2008, *CASTLES Survey*, <https://lweb.cfa.harvard.edu/castles/>
- Koopmans L. V. E., Bolton A., Treu T., Czoske O., Auger M. W., Barnabè M., Vegetti S., Gavazzi R., Moustakas L. A., Burles S., 2009, *ApJ Letters*, 703, L51
- Koopmans L. V. E., Treu T., Fassnacht C. D., Blandford R. D., Surpi G., 2003, *ApJ*, 599, 70
- Koposov S. E., Irwin M., Belokurov V., Gonzalez-Solares E., Yoldas A. K., Lewis J., Metcalfe N., Shanks T., 2014, *MNRAS*, 442, L85
- Koptelova E., Chen W. P., Chiueh T., Artamonov B. P., Oknyanskij V. L., Nuritdinov S. N., Burkhonov O., Akhunov T., Bruevich V. V., Ezhkova O. V., Gusev A. S., Sergeev A. V., Ehgamberdiev S. A., Ibragimov M. A., 2012, *A&A*, 544, A51
- Laureijs R., Amiaux J., Arduini S., Auguères J. L., Brinchmann J., Cole R., Cropper M., Dabin C., Duvet L., Ealet A., Garilli B., et al. 2011, *arXiv e-prints*, p. arXiv:1110.3193
- Lehár J., Falco E. E., Kochanek C. S., McLeod B. A., Muñoz J. A., Impey C. D., Rix H. W., Keeton C. R., Peng C. Y., 2000, *ApJ*, 536, 584
- Liddle A. R., 2004, *MNRAS*, 351, L49
- Liddle A. R., 2007, *MNRAS*, 377, L74
- Linder E. V., 2011, *PRD*, 84, 123529
- Lovell J. E. J., Jauncey D. L., Reynolds J. E., Wieringa M. H., King E. A., Tzioumis A. K., McCulloch P. M., Edwards P. G., 1998, *ApJ Letters*, 508, L51
- Melia F., 2007, *MNRAS*, 382, 1917
- Melia F., 2018, *MNRAS*, 481, 4855
- Melia F., 2020, *The Cosmic Spacetime*. Taylor and Francis, Oxford
- Melia F., 2023, *Pub Astron Soc Pacific*, in press (DOI:10.31219/osf.io/x23ek)
- Melia F., Shevchuk A. S. H., 2012, *MNRAS*, 419, 2579
- Meylan G., Courbin F., Lidman C., Kneib J. P., Tacconi-Garman L. E., 2005, *A&A*, 438, L37

- Millon M., Courbin F., Bonvin V., Buckley-Geer E., Fassnacht C. D., Frieman J., Marshall P. J., Suyu S. H., Treu T., Anguita T., Motta V., et al. 2020, *A&A*, 642, A193
- Millon M., Courbin F., Bonvin V., Paic E., Meylan G., Tewes M., Sluse D., Magain P., Chan J. H. H., Galan A., Joseph R., Lemon C., Tihhonova O., Anderson R. I., Marmier M., Chazelas B., Lendl M., Triaud A. H. M. J., Wyttenbach A., 2020, *A&A*, 640, A105
- Morgan C. W., Eyer M. E., Kochanek C. S., Morgan N. D., Falco E. E., Vuissoz C., Courbin F., Meylan G., 2008, *ApJ*, 676, 80
- Morgan C. W., Kochanek C. S., Dai X., Morgan N. D., Falco E. E., 2008, *ApJ*, 689, 755
- Oguri M., Inada N., Castander F. J., Gregg M. D., Becker R. H., Ichikawa S.-I., Pindor B., Brinkmann J., Eisenstein D. J., Frieman J. A., Hall P. B., et al. 2004, *Pub Astron Soc Japan*, 56, 399
- Oguri M., Inada N., Clocchiatti A., Kayo I., Shin M.-S., Hennawi J. F., Strauss M. A., Morokuma T., Schneider D. P., York D. G., 2008, *Astronomical Journal*, 135, 520
- Oguri M., Inada N., Hennawi J. F., Richards G. T., Johnston D. E., Frieman J. A., Pindor B., Strauss M. A., Brunner R. J., Becker R. H., Castander F. J., et al. 2005, *ApJ*, 622, 106
- Oguri M., Marshall P. J., 2010, *MNRAS*, 405, 2579
- Ostrowski F., McMahon R. G., Connolly A. J., Lemon C. A., Auger M. W., Banerji M., Hung J. M., Kuposov S. E., Lidman C. E., Reed S. L., Allam S., et al. 2017, *MNRAS*, 465, 4325
- Paraficz D., Hjorth J., 2009, *A&A*, 507, L49
- Petters A. O., Levine H., Wambsganss J., 2001, *Singularity theory and gravitational lensing*. Birkhäuser Verlag, Basel, Switzerland
- Planck Collaboration Aghanim N., Akrami Y., Ashdown M., Aumont J., Baccigalupi C., Ballardini M., Banday A. J., Barreiro R. B., Bartolo N., Basak S., et al. 2020, *A&A*, 641, A6
- Poindexter S., Morgan N., Kochanek C. S., Falco E. E., 2007, *ApJ*, 660, 146
- Rathna Kumar S., Stalin C. S., Prabhu T. P., 2015, *A&A*, 580, A38
- Rathna Kumar S., Tewes M., Stalin C. S., Courbin F., Asfandiyarov I., Meylan G., Eulaers E., Prabhu T. P., Magain P., Van Winckel H., Ehgamberdiev S., 2013, *A&A*, 557, A44
- Refsdal S., 1964, *MNRAS*, 128, 307
- Riess A. G., Yuan W., Macri L. M., Scolnic D., Brout D., Casertano S., Jones D. O., Murakami Y., Anand G. S., Breuval L., Brink T. G., et al. 2022, *ApJ Letters*, 934, L7
- Rusin D., Kochanek C. S., Keeton C. R., 2003, *ApJ*, 595, 29
- Schneider M. D., 2014, *PRL*, 112, 061301
- Schwarz G., 1978, *Annals of Statistics*, 6, 461
- Sergeyev A. V., Zheleznyak A. P., Shalyapin V. N., Goicoechea L. J., 2016, *MNRAS*, 456, 1948
- Shalyapin V. N., Goicoechea L. J., 2019, *ApJ*, 873, 117
- Shi K., Huang Y. F., Lu T., 2012, *MNRAS*, 426, 2452
- Sluse D., Claeskens J. F., Hutsemékers D., Surdej J., 2007, *A&A*, 468, 885
- Spiniello C., Sergeyev A. V., Marchetti L., Tortora C., Napolitano N. R., Shalyapin V., Agnello A., Getman F. I., Vaccari M., Serjeant S., Koopmans L. V. E., Baker A. J., Jarrett T. H., Covone G., Vernardos G., 2019, *MNRAS*, 485, 5086
- Suyu S. H., Auger M. W., Hilbert S., Marshall P. J., Tewes M., Treu T., Fassnacht C. D., Koopmans L. V. E., Sluse D., Blandford R. D., Courbin F., Meylan G., 2013, *ApJ*, 766, 70
- Takeuchi T. T., 2000, *Astrophys. Sp. Sci.*, 271, 213
- Tan M. Y. J., Biswas R., 2012, *MNRAS*, 419, 3292
- Treu T., Koopmans L. V., Bolton A. S., Burles S., Moustakas L. A., 2006, *ApJ*, 640, 662
- Treu T., Marshall P. J., 2016, *The Astronomy & Astrophysics Review*, 24, 11
- Tyson T., Wittman D., Hennawi J., Spergel D., 2002, in *APS April Meeting Abstracts APS Meeting Abstracts, LSST as a precision probe of dark energy*. p. Y6.004
- Verde L., Treu T., Riess A. G., 2019, *Nature Astronomy*, 3, 891
- Vuissoz C., Courbin F., Sluse D., Meylan G., Ibrahimov M., Asfandiyarov I., Stoops E., Eigenbrod A., Le Guillou L., van Winckel H., Magain P., 2007, *A&A*, 464, 845
- Wei J.-J., Wu X.-F., Melia F., 2014, *ApJ*, 788, 190
- Wisotzki L., Koehler T., Kayser R., Reimers D., 1993, *A&A*, 278, L15
- Wisotzki L., Schechter P. L., Chen H. W., Richstone D., Jahnke K., Sánchez S. F., Reimers D., 2004, *A&A*, 419, L31
- Wucknitz O., Biggs A. D., Browne I. W. A., 2004, *MNRAS*, 349, 14
- Yanagihara H., Ohmoto C., 2005, *Journal of Statistical Planning and Inference*, 133, 417